JOURNAL OF VIROLOGY, Sept. 2009, p. 8946–8956 Vol. 83, No. 17
0022-538X/09/$08.00+0 doi:10.1128/JVI.01857-08

Toll-Like Receptor 4 Deficiency Increases Disease and Mortality after Mouse Hepatitis Virus Type 1 Infection of Susceptible C3H Mice[▽]

Aaruni Khanolkar,[1]† Stacey M. Hartwig,[1]† Brayton A. Haag,[3] David K. Meyerholz,[2] John T. Harty,[1,3] and Steven M. Varga[1,3]*

Department of Microbiology, University of Iowa, Iowa City, Iowa 52242[1]; Department of Pathology, University of Iowa, Iowa City, Iowa 52242[2]; and Interdisciplinary Graduate Program in Immunology, University of Iowa, Iowa City, Iowa 52242[3]

Received 3 September 2008/Accepted 4 June 2009

Severe acute respiratory syndrome (SARS) is characterized by substantial acute pulmonary inflammation with a high mortality rate. Despite the identification of SARS coronavirus (SARS-CoV) as the etiologic agent of SARS, a thorough understanding of the underlying disease pathogenesis has been hampered by the lack of a suitable animal model that recapitulates the human disease. Intranasal (i.n.) infection of A/J mice with the CoV mouse hepatitis virus strain 1 (MHV-1) induces an acute respiratory disease with a high lethality rate that shares several pathological similarities with SARS-CoV infection in humans. In this study, we examined virus replication and the character of pulmonary inflammation induced by MHV-1 infection in susceptible (A/J, C3H/HeJ, and BALB/c) and resistant (C57BL/6) strains of mice. Virus replication and distribution did not correlate with the relative susceptibilities of A/J, BALB/c, C3H/HeJ, and C57BL/6 mice. In order to further define the role of the host genetic background in influencing susceptibility to MHV-1-induced disease, we examined 14 different inbred mouse strains. BALB.B and BALB/c mice exhibited MHV-1-induced weight loss, whereas all other strains of *H-2*^{b} and *H-2*^{d} mice did not show any signs of disease following MHV-1 infection. *H-2*^{k} mice demonstrated moderate susceptibility, with C3H/HeJ mice exhibiting the most severe disease. C3H/HeJ mice harbor a natural mutation in the gene that encodes Toll-like receptor 4 (TLR4) that disrupts TLR4 signaling. C3H/HeJ mice exhibit enhanced morbidity and mortality following i.n. MHV-1 infection compared to wild-type C3H/HeN mice. Our results indicate that TLR4 plays an important role in respiratory CoV pathogenesis.

Severe acute respiratory syndrome (SARS) is a disease that was initially observed in 2002 and led to approximately 8,000 affected individuals in multiple countries with over 700 deaths (1, 24, 47, 48). The causative agent of SARS was subsequently identified as a novel coronavirus (CoV) termed SARS-CoV (8, 17, 22, 27, 32, 37). Although SARS-CoV infections following the initial outbreak in 2002 and 2003 have been limited primarily to laboratory personnel, the identification of an animal reservoir for the virus raises concern about the potential for future outbreaks (25).

The pathogenesis of SARS has been difficult to study, in part because no animal model is able to fully recapitulate the morbidity and mortality observed in infected humans (35). Infection of a number of inbred mouse strains, including BALB/c, C57BL/6, and 129S, with primary human isolates of SARS-CoV results in the replication of the virus within the lung tissue without the subsequent development of readily apparent clinical disease (11, 16, 41). Infection of aged BALB/c mice results in clinically apparent disease that more closely mimics some aspects of SARS in humans (36). However, immune responses in aged mice are known to be altered (5, 15), and thus, the mechanisms that control the induction of disease may differ between adult and aged mice. Recent work has demonstrated that serial passage of SARS-CoV in mice results in a mouse adaptation that leads to more profound replication of the virus in the lung (28, 34). However, the time to death from this mouse-adapted SARS-CoV is 3 to 5 days, which is much more rapid than the time to mortality observed in fatal cases of SARS in humans.

Phylogenetic analysis has revealed that SARS-CoV is most closely related to group 2 CoVs, which include the mouse hepatitis virus (MHV) family (39). Thus, information gathered by infection of mice with closely related members of the group 2 CoVs may further contribute to our understanding of SARS-CoV pathogenesis in humans. While many strains of MHV induce primarily hepatic and central nervous system diseases (6, 7, 12, 18, 21, 23, 40), a recent study demonstrated that intranasal (i.n.) infection of A/J mice with MHV type 1 (MHV-1) induces pulmonary injury that shares several pathological characteristics with SARS-CoV infection of humans (2, 3, 9, 29, 43).

In the current study, we examined the relationship between MHV-1 replication in the lungs and the severity of disease in four inbred strains of mice: A/J, BALB/c, C57BL/6, and C3H/HeJ. Our results demonstrate that MHV-1 replicates to similar levels in the lung in each of these inbred strains of mice regardless of their relative levels of susceptibility, as measured by weight loss and clinical illness. Both A/J and C3H/HeJ mice exhibited enhanced weight loss and clinical illness following i.n. MHV-1 infection compared to BALB/c and C57BL/6 mice. Analysis of many different inbred mouse strains confirmed A/J

* Corresponding author. Mailing address: 3-532 Bowen Science Building, 51 Newton Road, University of Iowa, Iowa City, IA 52242. Phone: (319) 335-7784. Fax: (319) 335-9006. E-mail: steven-varga@uiowa.edu.

† A.K. and S.M.H. contributed equally to this work.

▽ Published ahead of print on 24 June 2009.

and C3H/HeJ mice as the most susceptible to i.n. MHV-1 infection. Interestingly, C3H/HeJ mice harboring a natural mutation in the gene that encodes Toll-like receptor 4 (TLR4) that disrupts its normal function exhibited greatly increased morbidity and mortality after i.n. MHV-1 infection compared to wild-type C3H/HeN mice. Our results indicate that TLR4 plays an important role in respiratory CoV pathogenesis.

MATERIALS AND METHODS

Mice. A/JCr, BALB/cAnNCr, C3H/HeJCr, C3H/HeNCr, and C57BL/6NCr mice were purchased from the National Cancer Institute (Frederick, MD). B10.BR-H2^k H2-T18^a/SgSnJ (B10.BR), B10.D2-Hc^0 H2^d H2-T18^c/oSnJ (B10.D2), CBA/J, C.B10-H2^b/LilMcdJ (BALB.B10), C.C3-H2^k/LilMcdJ (BALB.K), C57BL/10ScNCr, C57BL/10SnJ, DBA/2J, and NZB/BlNJ mice were purchased from The Jackson Laboratory (Bar Harbor, ME). Female mice aged 6 to 12 weeks were used for all experiments. The University of Iowa Animal Care and Use Committee approved all experimental procedures involving the use of animals.

Viruses and infection of mice. MHV-1 was purchased from the ATCC (Manassas, VA) and propagated in DBT cells. While under light anesthesia with isoflurane, mice were inoculated i.n. with 5×10^3 PFU of MHV-1 in a total volume of 50 μl. The weight of each mouse was determined and recorded daily. Each mouse was assessed a daily illness score based on the following scale: 0, no apparent illness; 1, slightly ruffled fur; 2, ruffled fur, active; 3, ruffled fur, inactive; 4, ruffled fur, inactive, hunched posture; 5, moribund or dead.

BAL and lung cell isolation. Collection of bronchoalveolar lavage (BAL) fluid and the preparation of single-cell suspensions from the BAL fluid and lung tissue were performed as previously described (30). Preparation and quantitation of lymphocytes in the BAL fluid were performed as previously described (30).

Intracellular-cytokine staining. Lung mononuclear cells (2×10^6 cells/ml) were stimulated with 50 ng/ml of phorbol myristate acetate (Sigma Aldrich, St. Louis, MO) and 500 ng/ml of ionomycin (Sigma) in the presence of 10 μg/ml of brefeldin A (Sigma) for 5 h at 37°C in RPMI 1640 medium (Gibco, Grand Island, NY) supplemented with 10% bovine growth serum (HyClone, Logan, UT), 10 U of penicillin G/ml, 10 μg of streptomycin sulfate/ml, 2 mM L-glutamine (Gibco), 5×10^{-5} M 2-mercaptoethanol, 1 mM sodium pyruvate (Gibco), 0.1 mM nonessential amino acids (Gibco), and 10 mM HEPES (Gibco). After incubation, the cells were blocked with purified anti-FcγRII/III monoclonal antibody (clone 93; eBioscience, San Diego, CA) and stained with monoclonal antibodies against CD4 (clone RM4-5; eBioscience) and CD8 (clone 53-6.7; eBioscience). Fluorescence-activated cell sorter lysing solution was used to fix the lung mononuclear cells and lyse the red blood cells. The cells were then washed with permeabilization buffer (staining buffer containing 0.5% saponin; Sigma) and stained with anti-gamma interferon (IFN-γ) monoclonal antibody (clone XMG1.2; eBioscience). The stained cells were analyzed on a FACSCanto (Becton Dickinson, San Jose, CA). Single-color controls were used for compensation. Lymphocytes were gated based on forward-scatter and side-scatter properties and were subsequently analyzed using FlowJo software (Tree Star Inc., Ashland, OR). Background staining was determined by using cells that were left unstimulated.

Histology. Whole lungs with the heart attached were harvested from mice at various time points after MHV-1 infection. The lungs were fixed in 10% neutral buffered formalin (Fisher Scientific, Pittsburgh, PA) prior to being processed and paraffin embedded at the University of Iowa Comparative Pathology Laboratory. The paraffin blocks were sectioned at 5-μm thickness. The sections were stained with hematoxylin and eosin at the University of Iowa Central Microscopy Core.

Histopathologic examination and scoring. A board-certified veterinary pathologist who was blinded to the study groups examined the tissue sections. Tissues were initially screened to define the breadth of morphological parameters that were of interest for subsequent histopathologic grading. Edema formation and cellular inflammation were graded (1 to 4 per animal) for distribution and severity in tissue sections. Histopathologic grading of lesions was modified from previous descriptions (4, 14, 38). The distribution of lesions was graded as follows: 1, absent to rare detection; 2, localized focus to multifocal, involving less than ~1/3 of the lung parenchyma; 3, multifocal to coalescing foci, involving ~1/3 to 2/3 of the lung parenchyma; and 4, coalescing to diffuse, involving more than ~2/3 of the lung parenchyma. Edema was defined as eosinophilic seroproteinaceous fluid within the alveolar lumen. The edema severity was graded as follows: 1, absent to rare detection; 2, mild, partially filling the alveoli with lacy to wispy fluid; 3, moderate, with partial filling of alveoli by pools of eosinophilic fluid; and 4, severe, with complete filling of alveoli by eosinophilic fluid with absence of detectable air space. During infection, pulmonary inflammation was primarily composed of lymphocytes, macrophages, and variable numbers of neutrophils. This infiltrate was localized to interstitial and perivascular spaces with a general lack of airway involvement. Accordingly, the severity of cellular infiltration was graded as follows: 1, absent to rare detection of interstitial inflammatory cells; 2, mild, with increased cellularity with minimal alteration of alveolar septa/interstitium thickness; 3, moderate, with increased cellularity of alveolar septa/interstitium with increased wall thickness and perivascular aggregates of inflammatory cells; 4, severe, with coalescing aggregates of perivascular inflammatory cells, increased cellularity and thickness of the alveolar septa/interstitium with increased inflammation "spillover" into the alveolar lumen. Total edema and total inflammation scores were assessed as the summation of the respective parameter distribution and severity grades.

Plaque assays. Whole lungs were harvested from MHV-1-infected A/J, BALB/c, C3H/HeJ, and C57BL/6 mice; weighed; and disrupted using an Ultra-Turrax T 25 basic homogenizer (IKA, Wilmington, NC). Supernatants were collected and stored at −80°C prior to further analysis. HeLa cells (ATCC) stably transfected with the MHV receptor (10) were grown in Dulbecco's modified Eagle's medium (DMEM) (Gibco, Grand Island, NY) supplemented with 10% fetal calf serum (FCS) (Atlanta Biologicals, Norcross, GA), 10 U/ml penicillin G (Gibco, Grand Island, NY), and 10 μg/ml streptomycin sulfate (Gibco). Serial dilutions of the supernatants were performed in serum-free DMEM (Gibco) supplemented as described above and subsequently incubated on HeLa cells expressing the MHV receptor for 30 min at 37°C. The plates were rocked every 10 min and overlaid overnight with 2 ml DMEM (Gibco) containing 10% FCS (Atlanta Biologicals) and supplemented as described above. The next day, the plates were stained with 2× minimal essential medium (Invitrogen, Carlsbad, CA) supplemented with 4% FCS (Atlanta Biologicals), 0.26% sodium bicarbonate (Gibco), 10 U/ml penicillin G (Gibco), 10 μg/ml streptomycin sulfate (Gibco), 1.8% SeaKem ME agarose (Cambrex, North Brunswick, NJ), and 0.01% neutral red (Sigma, St. Louis, MO). Plaques were counted after 2 to 4 h with the assistance of a light box.

Measurement of airway function. Airway function was measured in conscious, unrestrained, and spontaneously breathing mice using a barometric whole-body plethysmograph (Buxco Electronics, Wilmington, NC) as described previously (13). Baseline enhanced-pause (Penh) values for each mouse were averaged over 5 min and recorded prior to and on a daily basis following MHV-1 infection.

Statistics. All statistical analyses were performed using GraphPad (San Diego, CA) InStat software. Experiments involving three or more groups and demonstrating a Gaussian distribution were analyzed with a one-way analysis of variance (ANOVA) and a Bonferroni multiple-comparison posttest. Experiments with three or more groups that failed to demonstrate a Gaussian distribution were analyzed using a Kruskal-Wallis test and a Dunn multiple-comparison posttest. Experiments involving two groups with a Gaussian distribution were analyzed using an unpaired *t* test. Survival data were analyzed using a Mantel-Cox log rank test. A P value of <0.05 was considered significant.

RESULTS

MHV-1 replication in the lungs does not correlate with weight loss and systemic disease. Since A/J and C3H/St mice infected with MHV-1 exhibited increased mortality compared to BALB/cJ and C57BL/6J mice (2), we first determined if relative susceptibility was correlated with enhanced weight loss and signs of overt clinical illness, such as ruffled fur, inactivity, and a hunched posture. The mice were weighed and scored for illness daily for 9 days following i.n. infection with 5×10^3 PFU of MHV-1. A/J and C3H/HeJ mice exhibited extensive weight loss between days 3 and 9 postinfection (p.i.) (Fig. 1A). In addition, both strains of mice exhibited high mortality rates between days 7 and 9 p.i. In contrast, BALB/c mice lost a moderate amount of weight between days 2 and 3 p.i., with slow recovery evident over the next 6 days. C57BL/6 mice exhibited no weight loss following MHV-1 infection.

The mice were also monitored daily for overt signs of clinical illness. A/J and C3H/HeJ mice first exhibited signs of clinical illness by days 2 and 3 after infection with MHV-1, respectively, that increased in severity through day 9 p.i. (Fig. 1B).

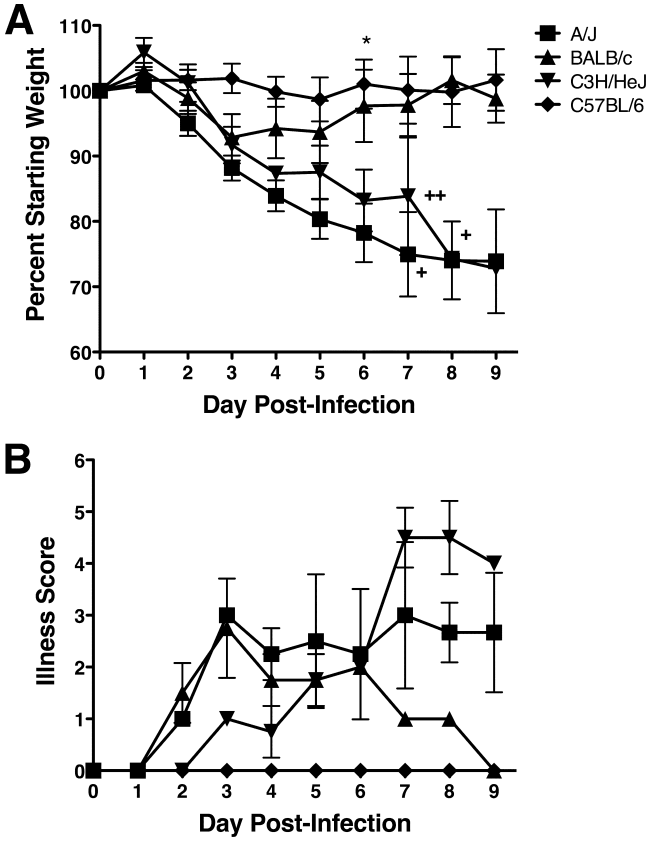

FIG. 1. MHV-1-induced weight loss and systemic disease. (A) A/J, BALB/c, C3H/HeJ, and C57BL/6 mice were infected i.n. with MHV-1, and their weights were monitored daily. The results are depicted as the mean percentage of the starting weight ($n = 4$ mice per group). The error bars indicate the standard errors of the mean (SEM). The experiment was performed twice with similar results. Each plus represents the loss of an individual mouse on the indicated day. *, $P < 0.05$ for A/J versus BALB/c and C57BL/6 mice as determined by ANOVA. (B) The mice shown in panel A were observed daily and assigned a clinical illness score as described in Materials and Methods. The results are expressed as the mean illness score ($n = 4$ mice per group). The error bars indicate the SEM.

BALB/c mice exhibited moderate clinical illness between days 2 and 8 p.i., whereas C57BL/6 mice never exhibited any signs of clinical illness following MHV-1 infection.

To determine if the magnitude of MHV-1 replication in the lungs was correlated with the relative amount of weight loss and systemic illness, lung virus titers were determined at days 4, 9, 14, and 21 p.i. The amount of virus recovered from the lung did not correlate with either weight loss or the development of clinical illness (Fig. 2). At day 4 p.i., all four strains of mice exhibited high titers of MHV-1 in the lungs, with A/J mice exhibiting significantly ($P < 0.05$) higher virus titers than C3H/HeJ mice. There was no significant ($P > 0.05$) difference in the virus titers between A/J mice and either BALB/c or C57BL/6 mice. Interestingly, C57BL/6 mice, which did not exhibit weight loss or show any signs of clinical illness, had levels of virus that were not statistically different ($P > 0.05$) than those of C3H/HeJ and BALB/c mice, which both exhibited weight loss and clinical disease at this time point (Fig. 1). Titers in the lung dropped by 10- to 100-fold by day 9 p.i., remaining low but detectable in the lungs of some BALB/c and C57BL/6 mice through day 21 p.i. A/J and C3H/HeJ mice exhibited high mortality rates between days 7 and 10 p.i.; however, virus titers measured from the surviving mice at days 9, 14, and 21 p.i. did not differ significantly from those of either BALB/c or C57BL/6 mice. Virus replication was also examined in the spleen, liver, and brain. Small amounts of virus could be recovered from the spleen and brain at day 4 p.i. and subsequently fell below detection limits by day 9 p.i. in all four strains of mice. Low virus titers were also observed in the liver in all four strains of mice through day 9 p.i., subsequently decreasing below the limit of detection by day 21 p.i. (data not shown). These results indicate that the relative severity of MHV-1-induced disease does not correlate with the virus titer.

Histological examination of lung sections. Lungs from A/J, BALB/c, C3H/HeJ, and C57BL/6 mice infected with MHV-1 were harvested at days 5, 7, and 9 p.i. and stained with hematoxylin-eosin. Figure 3A to D shows a representative section taken at day 9 p.i. from each strain of mice at low power to demonstrate the relative amount of edema that developed in the lungs of each strain. In all mouse strains examined, MHV-1 infection induced a diffuse mononuclear cell infiltration in the lungs that was primarily localized to interstitial and perivascular spaces with a general lack of airway involvement. We did not observe significant strain-dependent differences in the distribution of inflammatory cells in the lung. However, A/J and C3H/HeJ mice exhibited more prominent pathological changes in the lung, including hyaline membrane formations, syncytia, fibrin depositions, cellular necrosis, and severe pulmonary edema (Fig. 3E to H). A/J mice exhibited significantly higher ($P < 0.05$) total inflammatory scores at days 5 and 9 p.i. than C57BL/6 mice (Fig. 4A). We did observe increased edema in A/J and C3H/HeJ mice that had survived to day 9 p.i. compared to BALB/c and C57BL/6 mice, neither of which exhibited either signs of clinical disease or weight loss at this time point (Fig. 4B). In particular, at day 9 p.i., C57BL/6 mice exhibited significantly less ($P < 0.05$) total edema than either A/J or C3H/HeJ mice. Our results demonstrate that both A/J and C3H/HeJ mice develop increased MHV-1-induced pulmonary edema compared to BALB/c and C57BL/6 mice.

Magnitude and kinetics of pulmonary inflammation. The increased morbidity and mortality exhibited by A/J and C3H/HeJ mice occurred during the time frame when a virus-specific adaptive immune response would develop. Therefore, we next determined the magnitude and examined the character of the pulmonary inflammation induced by MHV-1 infection. To determine more precisely the relative magnitude of the pulmonary inflammation induced by MHV-1 infection, we examined the cellularity in the BAL fluid and lung parenchyma. Increasing numbers of mononuclear cells were observed in the BAL fluid between days 5 and 9 p.i. in all strains (Fig. 5A). In contrast, total mononuclear cell counts in the lungs of A/J, BALB/c, and C57BL/6 mice were similar between days 5 and 9 p.i., whereas C3H/HeJ mice exhibited a sharp increase in the number of mononuclear cells at days 7 to 9 p.i. (Fig. 5B). Examination of the character of the inflammatory cells within the BAL fluid of BALB/c and C57BL/6 mice revealed that the majority of the infiltrating cells were lymphocytes and macrophages (Fig. 6A to C). In contrast, A/J mice showed a higher proportion of neutrophils at day 5 p.i., which subsequently

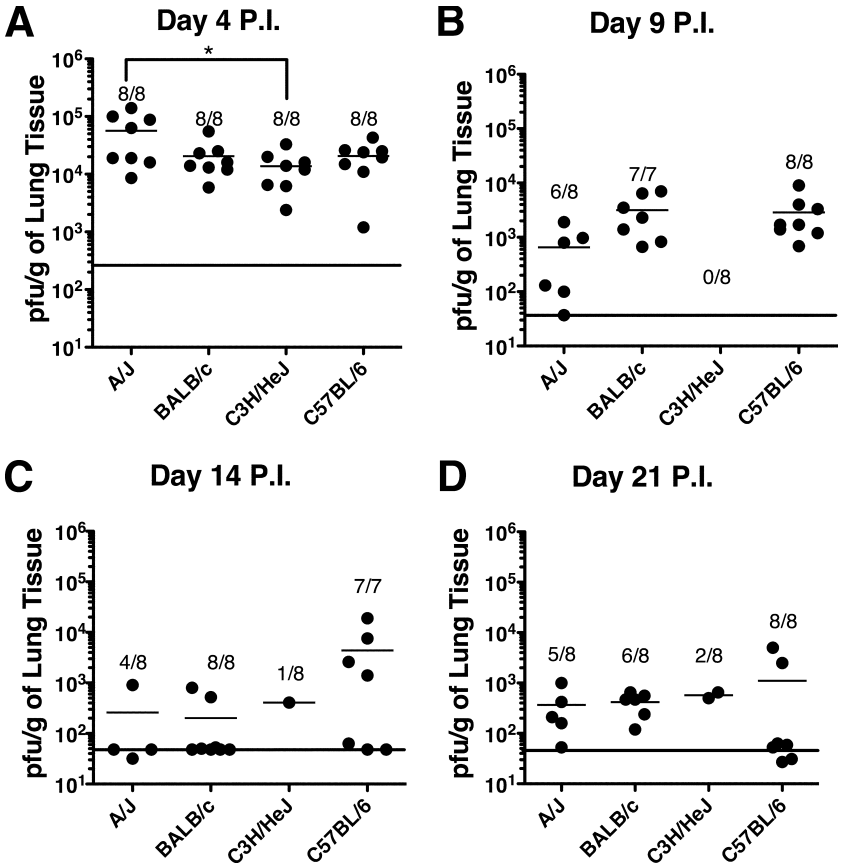

FIG. 2. Kinetics of MHV-1 replication in the lungs. The data represent the PFU/g of lung tissue for individual mice of the indicated strains at days 4 (A), 9 (B), 14 (C), and 21 (D) p.i. with MHV-1. The mean of each group is indicated by a short horizontal line. The fractions represent the number of surviving mice over the number of initial mice for each strain at each time point. The limit of detection at each time point is indicated by the long horizontal line. Combined data from two independent experiments are shown ($n = 7$ to 8 mice per group). *, $P < 0.05$ for A/J versus C3H/HeJ mice as determined by ANOVA.

declined by days 7 and 9 p.i. Interestingly, a high proportion of neutrophils were found in the BAL of C3H/HeJ mice at all time points examined. These results indicate that the increased severity of disease exhibited by A/J and C3H/HeJ mice is not the result of an increased magnitude of pulmonary inflammation compared to BALB/c and C57BL/6 mice.

Airway function. To determine the effect of MHV-1 infection on airway function, we monitored baseline Penh in A/J, BALB/c, C3H/HeJ, and C57BL/6 mice between days 3 and 7 following i.n. MHV-1 infection. A/J mice exhibited elevated baseline Penh between days 3 and 7 p.i. (Fig. 7). C3H/HeJ mice exhibited increased Penh relative to BALB/c and C57BL/6 mice starting between days 5 and 7 p.i. BALB/c and C57BL/6 mice exhibited only small or no increases in Penh between days 3 and 5 p.i., consistent with the clinical measures described above (Fig. 1). Thus, our results demonstrate that both A/J and C3H/HeJ mice exhibit increased Penh following acute MHV-1 infection compared to BALB/c and C57BL/6 mice.

Relative MHV-1 susceptibilities of inbred mice. We sought to further define the host genetic factors that mediate susceptibility to MHV-1-induced disease in inbred mice. To examine both major histocompatibility complex (MHC)-linked, and non-MHC-linked factors, disease severity was evaluated in 10 additional strains of inbred mice to determine their relative susceptibilities to i.n. MHV-1 infection. C57BL/6 mice ($H\text{-}2^b$ MHC) were resistant to MHV-1-induced disease as measured by weight loss (Fig. 8A). In contrast, BALB.B10 mice (also $H\text{-}2^b$ MHC, with BALB/c background genes) exhibited a moderate amount of weight loss early (days 3 and 4) after infection followed by rapid recovery. Among strains of mice expressing the MHC $H\text{-}2^d$ haplotype, BALB/c mice lost approximately 10% of their starting weight by day 3 p.i., gradually recovering weight over the next 2 weeks (Fig. 8B). B10.D2, DBA/2J, and NZB/BlNJ mice failed to lose substantial weight following MHV-1 infection, indicating that they are resistant to MHV-1-induced weight loss. Among $H\text{-}2^k$ mice, CBA/J and B10.BR mice exhibited moderate weight loss between days 3 and 9 p.i. Moreover, like BALB/c and BALB.B10 mice, BALB.K mice exhibited a moderate loss of weight between days 3 and 5 p.i., rebounding quickly afterwards. As expected, infection of the mixed MHC haplotype A/J mice also resulted in rapid weight loss and high mortality. The above-mentioned results indicate that most strains expressing either the $H\text{-}2^b$ or the $H\text{-}2^d$ MHC haplotype are resistant to MHV-1-induced disease. Strains that carry the BALB/c background genes exhibit moderate susceptibility to MHV-1-induced weight loss independent of their MHC disposition. All mice expressing $H\text{-}2^k$ MHC haplotypes exhibit moderate susceptibility to MHV-1induced weight loss

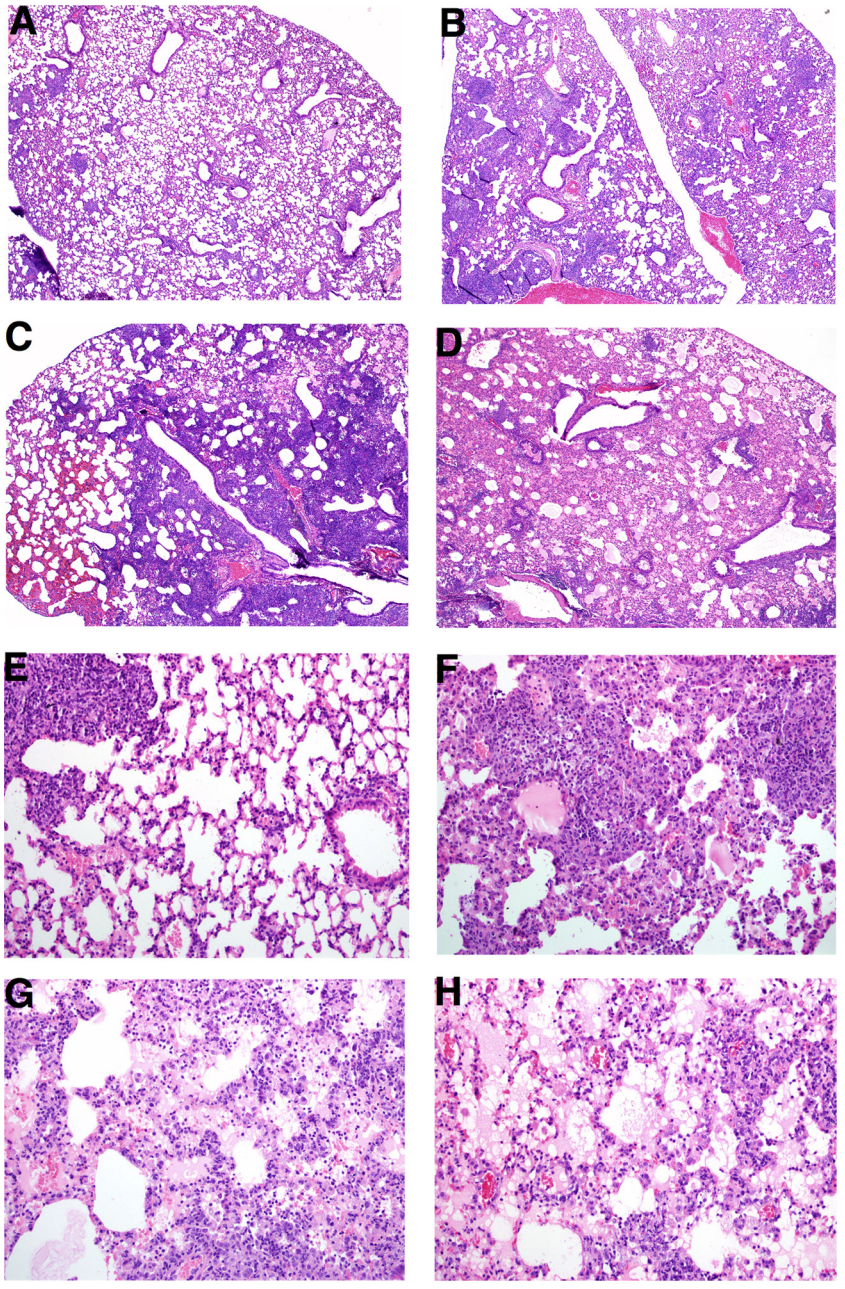

FIG. 3. Hematoxylin and eosin staining of lung sections. Whole lungs from C57BL/6 (A and E), BALB/c (B and F), A/J (C and G), and C3H/HeJ (D and H) mice were harvested at day 9 p.i. with MHV-1. The lungs were fixed in 10% neutral buffered formalin, embedded in paraffin, and sectioned prior to being stained with hematoxylin and eosin. Final magnification, ×40 (A to D) and ×200 (E to H). The images are representative of lung sections obtained from two separate experiments (n = 5 to 8 mice per group).

independent of their background genes. Thus, these results indicate that both MHC-linked and non-MHC-linked genes can contribute to susceptibility to MHV-1-induced disease.

Because C3H/HeJ mice lack a functional TLR4 gene, we wanted to further assess the role of TLR4 in susceptibility to MHV-1-induced disease. We first examined either wild-type or TLR4-deficient mice on the C57BL/10 (*H-2*^{b} MHC haplotype) background. Like C57BL/6 mice, C57BL/10SnJ mice were resistant to MHV-1-induced weight loss (Fig. 9A). C57BL/10ScN mice, which are homozygous for a null mutation of the TLR4 gene (31, 45), did not exhibit weight loss that was significantly different from that of C57BL/10SnJ mice. Thus, TLR4 deficiency does not render a resistant strain susceptible to MHV-1-induced disease. We next examined the effect of TLR deficiency within the susceptible C3H *H-2*^{k} mice. C3H/HeJ mice lost approximately 20% of their body weight by day 8 p.i. (Fig. 9B). In addition, C3H/HeJ mice also exhibited a high mortality rate, with the majority of the mice dying between days 7 and 10 p.i. C3H/HeN mice (wild-type TLR4) followed a weight loss trend similar to that of C3H/HeJ mice during the first 7 days of

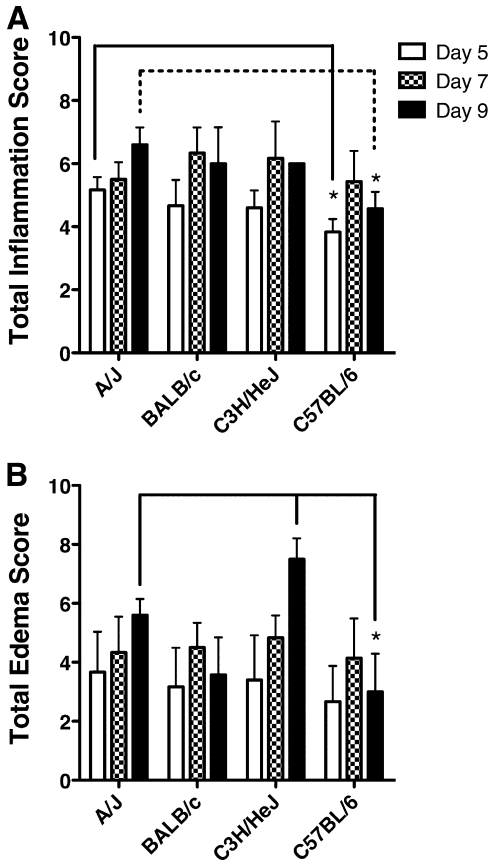

FIG. 4. Pulmonary inflammation. Whole lungs were harvested at day 5, day 7, and day 9 after MHV-1 infection for each of the indicated mouse strains. The lungs were fixed in 10% neutral buffered formalin, embedded in paraffin, and sectioned prior to being stained with hematoxylin and eosin. The slides were scored for total inflammation (A) and total edema (B) according to the scales described in Materials and Methods. The results from two combined experiments are expressed as the mean of a total five to eight mice per group. The error bars indicate the standard deviations. *, $P < 0.05$ as determined by ANOVA for the comparisons indicated.

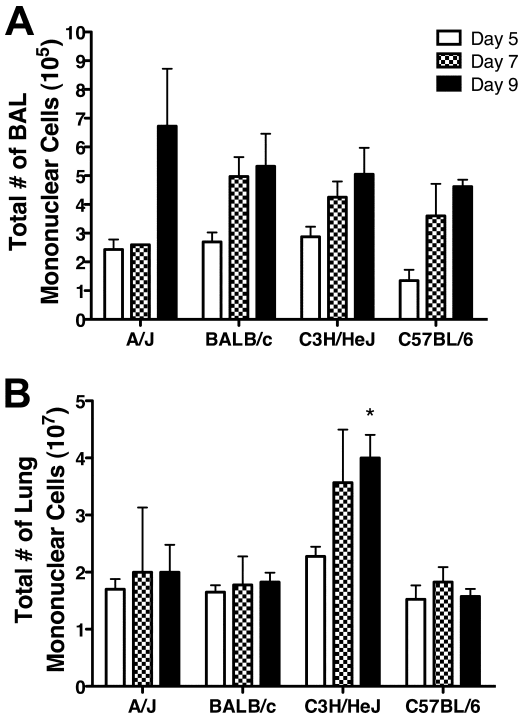

FIG. 5. Tempo of pulmonary inflammation. BAL fluid and lung cells were harvested on day 5, day 7, and day 9 after MHV-1 infection for each of the indicated mouse strains. Total mononuclear cells in the BAL fluid (A) and lung (B) were counted using a hemocytometer. The results are expressed as the mean of four mice per group. The error bars indicate the standard deviations. The experiment was performed twice with similar results. *, $P < 0.05$ for day 9 C3H/HeJ mice versus day 9 A/J, day 9 BALB/c, and day 9 C57BL/6 mice as determined by ANOVA.

infection, but C3H/HeN mice then exhibited more robust recovery than C3H/HeJ mice. These results indicate that TLR4 deficiency increases susceptibility to MHV-1-induced disease within C3H mice.

Role of TLR4 in susceptibility to MHV-1-induced disease. The results described above show, most remarkably, marked differences in mortality between the C3H/HeJ mice that lacked a functional TLR4 gene and their C3H/HeN controls that contained a fully functional TLR4 gene. C3H/HeJ mice exhibited an approximately 70% mortality rate by day 14 p.i., whereas C3H/HeN mice exhibited only 20% mortality during this time frame (Fig. 10). Increased mortality was not associated with an increase in virus replication in the lung, as virus titers were not significantly different between the C3H/HeJ and C3H/HeN mice at day 4 or 7 p.i. (data not shown). TLR4 has recently been implicated as an important factor in controlling the development of acute lung injury (20). Therefore, we monitored Penh daily in C3H/HeJ and C3H/HeN mice following i.n. MHV-1 infection. Surprisingly, C3H/HeN mice exhibited increased baseline Penh compared to C3H/HeJ mice between days 2 and 7 p.i. (Fig. 11). These results demonstrate that despite exhibiting improved airway function, C3H/HeJ mice that lacked a functional TLR4 gene exhibited increased susceptibility to MHV-1-induced morbidity and mortality.

The cell types that trafficked into the lungs of wild-type C3H/HeN and TLR4-deficient C3H/HeJ mice were examined by flow cytometry at days 5 and 7 following acute MHV-1 infection (Fig. 12). No significant differences were observed for $CD4^+$ $CD3^+$ or $CD8^+$ $CD3^+$ T cells or $CD19^+$ $CD3^-$ B cells. C3H/HeJ mice exhibited increased total numbers of NK cells ($DX\text{-}5^+$ $CD3^-$ cells; $P < 0.05$ at day 7 only), neutrophils ($CD11b^+$ $CD11c^-$ $Ly6C^+$ $Ly6G^+$ cells; $P < 0.05$ at day 5 only), and alveolar macrophages ($CD11b^+$ $CD11c^+$ MHC class II^{low} Siglec F^+ cells). These results suggest that C3H/HeJ mice exhibit increased numbers of pulmonary NK cells and granulocytes following acute MHV-1 infection compared to wild-type C3H/HeN mice.

We next sought to determine if the adaptive immune response to MHV-1 was altered in TLR4-deficient mice in order to better understand the enhanced mortality observed in mice that lacked functional TLR4 signaling. Because the immunodominant T-cell epitopes are not currently defined for MHV-1, we quantified the frequency of CD4 and CD8 T cells capable of making IFN-γ following stimulation with phorbol myristate acetate and ionomycin. We compared the total numbers of

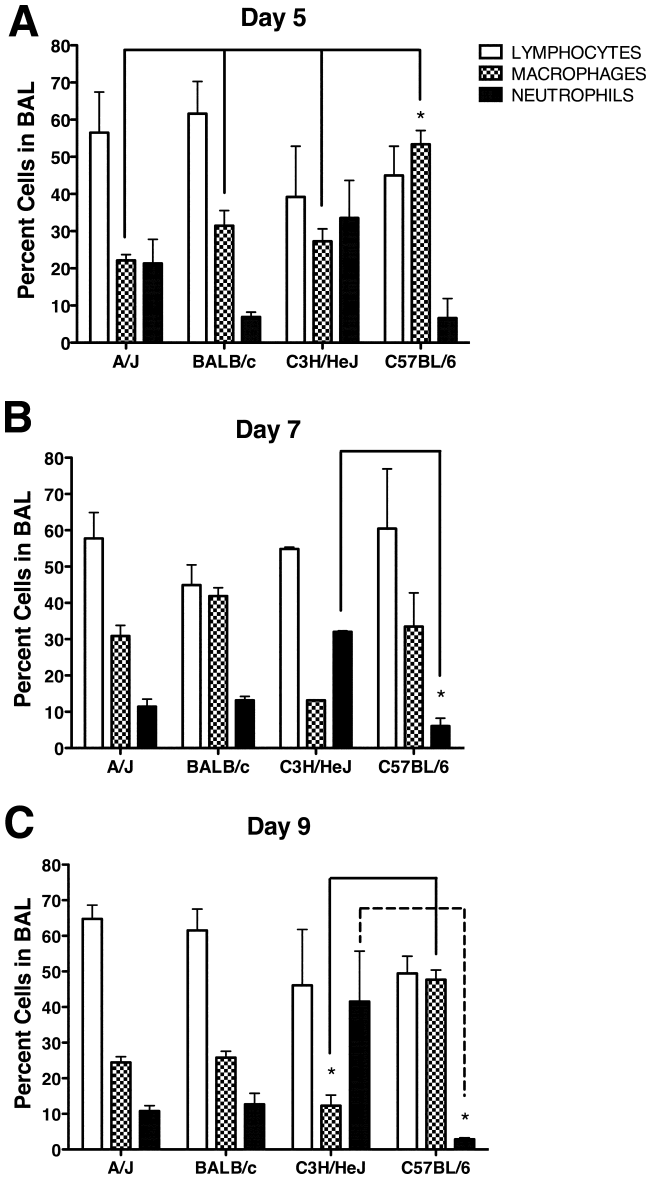

FIG. 6. Character of the pulmonary inflammation. BAL was performed at day 5 (A), 7 (B), or 9 (C) after MHV-1 infection. BAL fluid cells were cytospun and subsequently stained with Diff-Quik. The percentages of lymphocytes, macrophages, and neutrophils were determined from counts obtained under a light microscope. No eosinophils were observed in any of the mice. The results are expressed as the mean of four mice per group. The error bars indicate the standard deviations. The experiment was performed twice with similar results. *, $P < 0.05$ as determined by ANOVA for the comparisons indicated.

IFN-γ-producing cells in the lung at day 7 after MHV-1 infection of C3H/HeN versus C3H/HeJ mice (Fig. 13). C3H/HeJ mice had a significantly ($P < 0.05$) higher total number of IFN-γ-producing CD4 T cells in the lung than C3H/HeN mice. The two strains had similar total numbers of IFN-γ-producing CD8 T cells in the lung at this time point. These results indicate that in the absence of signals through TLR4, the CD4 T-cell response in the lung is increased following MHV-1 infection of C3H mice, which may contribute to enhanced morbidity and mortality.

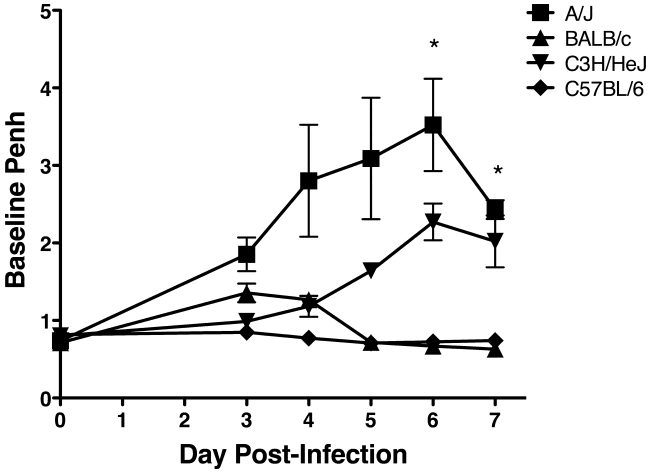

FIG. 7. MHV-1-induced alterations in airway function. Penh was determined by whole-body plethysmography and assessed daily after i.n. MHV-1 infection of A/J, BALB/c, C3H/HeJ, and C57BL/6 mice. The results are expressed as the mean baseline Penh for three or four mice per group. The error bars indicate the standard errors of the mean. The experiment was performed twice with similar results. *, $P < 0.05$ for A/J versus BALB/c and C57BL/6 mice as determined by ANOVA.

DISCUSSION

The underlying immune mechanisms that contribute to the development of SARS in humans remain poorly understood, in part because few cases of the disease have occurred since the initial outbreak in 2002 and 2003. Mice represent an excellent model system for the study of virus-host interactions due to the generation of inbred strains of mice and the ability to manipulate the genome. Thus, the successful development of a small-animal model that closely resembles the key pathological findings of the human disease would significantly improve our ability to examine the pathogenesis of SARS. However, to date, no animal model fully recapitulates the morbidity and mortality observed in infected humans (36).

A recent report examined the abilities of several MHV strains to produce productive infections in the lung following i.n. administration (2). MHV-1 was shown to replicate in the lung and produce pulmonary pathology in A/J mice that shared several key characteristics with the lung pathology noted in human SARS cases (3, 9, 29, 43). In the current study, we examined the disease induced by i.n. administration in several strains of mice and showed that i.n. infection of A/J and C3H/HeJ mice resulted in increased weight loss, clinical illness, and Penh compared to either BALB/c or C57BL/6 mice. Several observations indicate that the adaptive immune response may play an important role in the enhanced morbidity and mortality we observed in A/J and C3H/HeJ mice. First, BALB/c mice mirror the weight loss observed early after MHV-1 infection of A/J and C3H/HeJ mice. However, by day 5 p.i., when the adaptive immune response would start to become apparent, BALB/c mice start to regain weight whereas A/J and C3H/HeJ mice continue to lose weight. In addition, our preliminary data indicate that depletion of both CD4 and CD8 T cells prevents MHV-1-induced mortality in either A/J or C3H/HeJ mice (A. Khanolkar, S. M. Hartwig, S. M. Varga, and J. T. Harty, un-

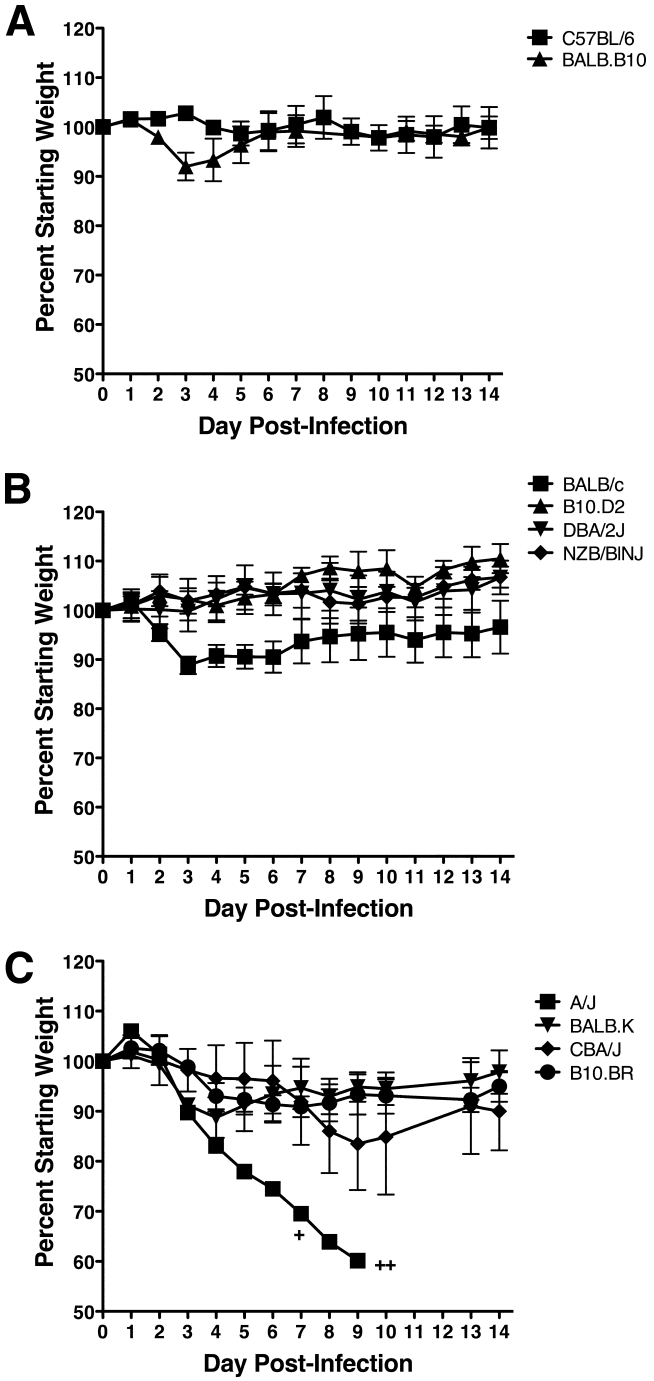

FIG. 8. MHV-1-induced weight loss in congenic strains of mice. *H-2*^{b} C57BL/6 and BALB.B10 (A); *H-2*^{d} BALB/c, B10.D2, DBA/2J, and NZB/BINJ (B); and *H-2*$^{d/k}$ A/J and *H-2*^{k} BALB.K, CBA/J, and B10.BR (C) mice were infected i.n. with MHV-1, and their weights were monitored daily. Each plus represents the loss of an individual mouse on the indicated day. The results are expressed as the mean percentage of the starting weight for three or four mice per group. The error bars indicate the standard deviations. The experiment was performed twice with similar results.

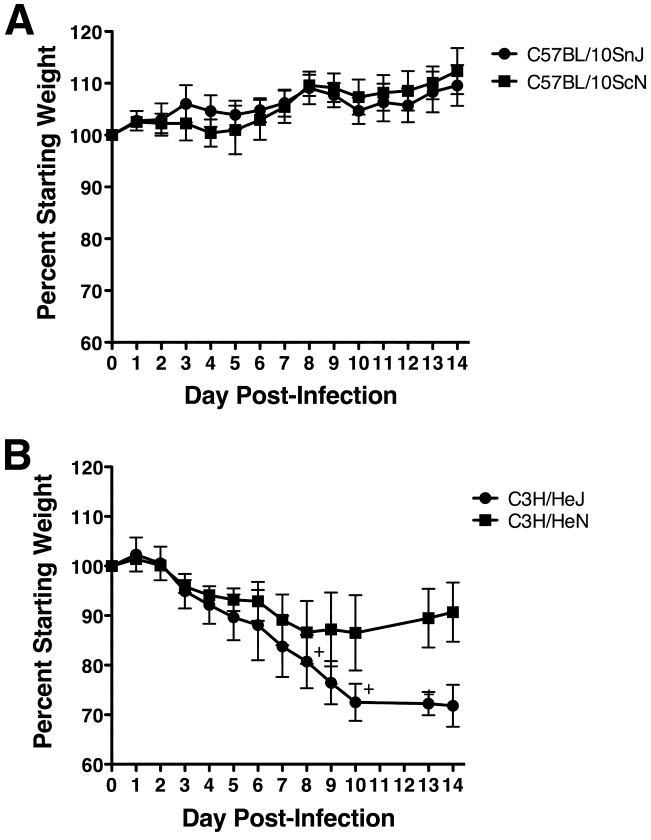

FIG. 9. TLR4 deficiency enhances the susceptibility of C3H mice to MHV-1-induced weight loss. *H-2*^{b} C57BL/10SnJ and C57BL/10ScNCr (A) and *H-2*^{k} C3H/HeJCr and C3H/HeNCr (B) mice were infected i.n. with MHV-1, and their weights were monitored daily. Weight loss was not recorded on days 11 and 12 in panel B. Each plus represents the loss of an individual mouse on the indicated day. The results are expressed as the mean percentage of the starting weight for four mice per group. The error bars indicate the standard deviations. The experiment was performed twice with similar results.

published data). The factors that drive the weight loss in A/J and C3H/HeJ mice are currently unknown; however, the cytokine tumor necrosis factor alpha (TNF-α) represents a likely candidate. Macrophages and T cells are the primary producers of TNF-α, and when it is released in large quantities, TNF-α production has been associated with cachexia in mice. Antibody-mediated TNF-α depletion has been shown to ameliorate the weight loss observed following infection with either respiratory syncytial virus (RSV) or influenza virus (19). Thus, TNF-α likely contributes to the development of weight loss following MHV-1 infection; however, this has yet to be formally tested.

Although MHV strains can cause mortality associated with liver disease, we do not believe A/J and C3H/HeJ mice were succumbing to liver disease. Infection of either A/J or C3H/HeJ mice with a higher dose (2×10^5 PFU) of MHV-1 administered intraperitoneally does not induce disease or mortality in either mouse strain. In addition, we also examined the liver via histology during the course of these studies, and we did not find liver pathology that would be consistent with the time frame during which our mice succumbed to the infection (data not shown).

The increased mortality observed in the A/J and C3H/HeJ mice appears to be primarily due to respiratory failure caused by severe pulmonary edema. A recent study suggests that sig-

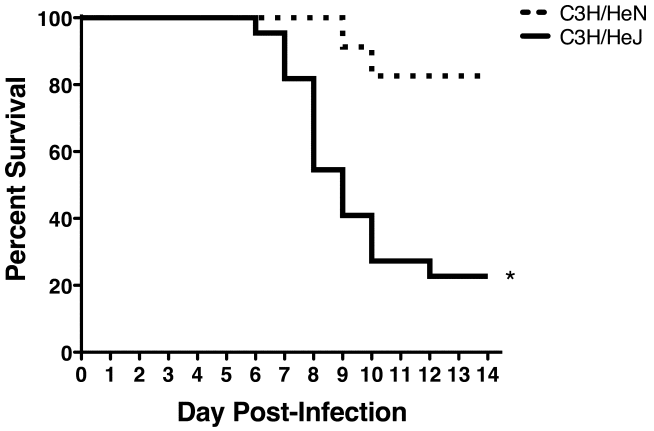

FIG. 10. TLR4 deficiency enhances susceptibility to MHV-1-induced mortality. Wild-type C3H/HeN and TLR4-deficient C3H/HeJ mice were monitored daily after i.n. MHV-1 infection. The cumulative results from six separate experiments representing 25 C3H/HeN mice and 22 C3H/HeJ mice are shown. The data are plotted as a Kaplan-Meier survival curve. *, $P < 0.0001$ for C3H/HeN versus C3H/HeJ as determined by a Mantel-Cox log rank test.

naling through TLR4 may be critical for the induction of oxidative stress and the subsequent development of acute lung injury (20). TLR4-deficient mice were found to be resistant to increased lung elastance and pulmonary edema following either acid-induced or inactivated H5N1 influenza virus-induced acute lung injury (20). Consistent with findings reported by Imai et al. (20), we observed that TLR4-deficient mice exhibited improved lung function compared to wild-type controls (Fig. 11).

TLR4 polymorphisms in humans have been linked to an increase in disease severity following infection with RSV (26, 33, 42). However, the mechanism that controls this disease enhancement following RSV infection is currently not well

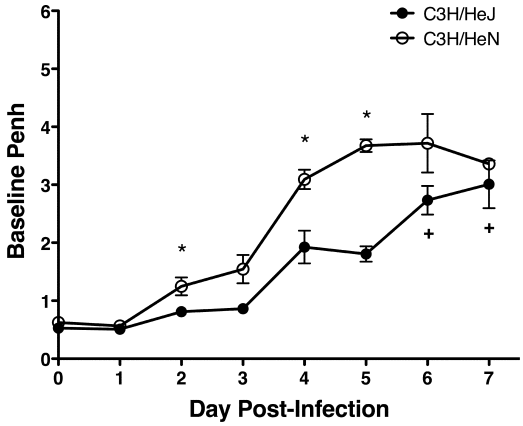

FIG. 11. Improved airway function in TLR4-deficient mice following acute MHV-1 infection. Wild-type C3H/HeN and TLR4-deficient C3H/HeJ mice were infected i.n. with MHV-1. The mice were monitored daily by whole-body plethysmography. Each plus represents the loss of an individual mouse on the indicated day. The results are expressed as the mean baseline Penh for four mice per group. The error bars indicate the standard errors of the mean. The experiment was performed twice with similar results. *, $P < 0.05$ for C3H/HeN versus C3H/HeJ mice as determined by Student's t test.

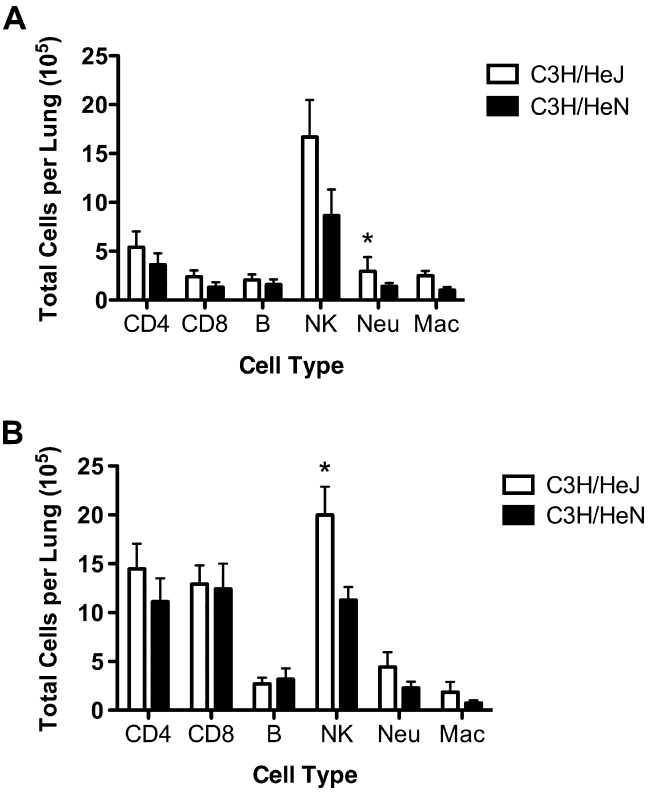

FIG. 12. Effect of TLR4 deficiency on MHV-1-induced pulmonary infiltrates. Wild-type C3H/HeN and TLR4-deficient C3H/HeJ mice were infected i.n. with MHV-1. Lung mononuclear cells were harvested on day 5 (A) and day 7 (B) after MHV-1 infection for each of the indicated strains. The results are expressed as the mean total number of the indicated cell type per lung for seven mice per group on day 5 and eight mice per group on day 7. The error bars indicate the standard errors of the mean. The experiment was performed twice with similar results. *, $P < 0.05$ for C3H/HeN versus C3H/HeJ mice as determined by Student's t test.

understood. We found that TLR4-deficient mice exhibited increased mortality following i.n. MHV-1 infection compared to wild-type controls. The C3H/HeJ mice succumbed to the infection primarily between days 7 and 10 p.i., suggesting that the TLR4 deficiency impacted a critical event influencing the adaptive immune response that led to the death of these mice. Consistent with a role for the adaptive immune response in mediating the enhanced mortality observed in C3H/HeJ mice, we demonstrated that the total number of IFN-γ-producing CD4 T cells is significantly increased in C3H/HeJ mice compared to C3H/HeN mice (Fig. 13).

Consistent with previous work, our results indicate that the genetic background of the host exerts a profound effect on susceptibility to MHV-1-induced disease. C57BL/6 and C57BL/10 mice are extremely resistant to MHV-1-induced disease. TLR4-deficient C57BL/10ScN did not exhibit any increase in MHV-1-induced morbidity. Our results indicate that the host genetic background influences the requirement for TLR4-mediated signals during MHV-1 infection and that the genetic influences that result in resistance to MHV-1-induced disease are dominant over the requirement for TLR4-mediated signals.

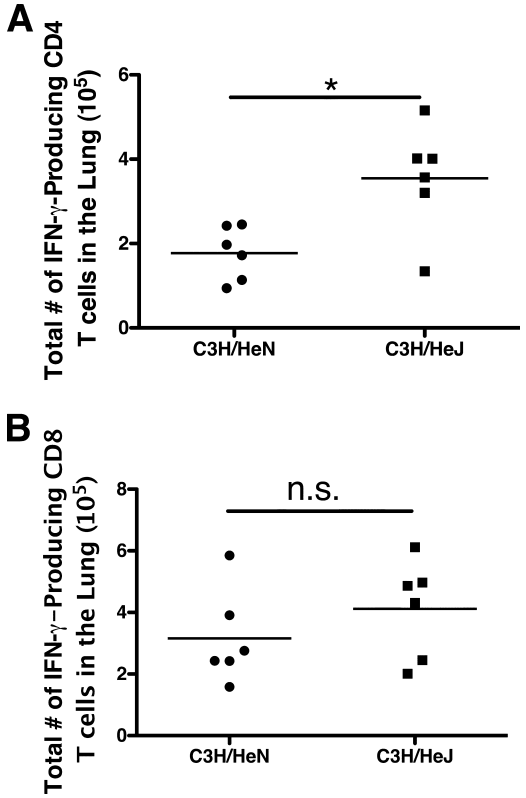

FIG. 13. Increased CD4 T-cell responses in TLR4-deficient mice following acute MHV-1 infection. Lung mononuclear cells were harvested from wild-type C3H/HeN and TLR4-deficient C3H/HeJ mice on day 7 after MHV-1 infection. The cells were stimulated with phorbol myristate acetate and ionomycin for 5 h in the presence of brefeldin A prior to being fixed, permeabilized, and stained for CD4, CD8, and IFN-γ. The total numbers of IFN-γ-producing CD4 (A) and CD8 (B) T cells within the lung for each individual are shown. The results represent two combined experiments with six mice per group. The horizontal line indicates the mean. *, $P < 0.05$ as determined by Student's *t* test. n.s., not significantly different ($P > 0.05$).

With the identification of several new CoVs within the last few years, including SARS-CoV (1, 24, 47, 48), human CoV HKU1 (46), and human CoV NL63 (44), it has become increasing apparent that CoVs can be the cause of significant virus-induced respiratory disease in humans. However, studies examining the immunobiology of CoV infections in the respiratory tract remain scarce. Mice infected i.n. with MHV-1 represent an excellent model of CoV-induced lung injury that may provide additional insights into the pathogenesis of CoV infection in humans.

ACKNOWLEDGMENTS

We thank Stanley Perlman for critical review of the manuscript.

This work was supported by National Institutes of Health Program Project Grant P01 AI-060699 (to J.T.H. and S.M.V.) and the University of Iowa Department of Pathology (to D.K.M.).

REFERENCES

1. **Anonymous.** 2003. A multicentre collaboration to investigate the cause of severe acute respiratory syndrome. Lancet **361:**1730–1733.
2. **De Albuquerque, N., E. Baig, X. Ma, J. Zhang, W. He, A. Rowe, M. Habal, M. Liu, I. Shalev, G. P. Downey, R. Gorczynski, J. Butany, J. Leibowitz, S. R. Weiss, I. D. McGilvray, M. J. Phillips, E. N. Fish, and G. A. Levy.** 2006. Murine hepatitis virus strain 1 produces a clinically relevant model of severe acute respiratory syndrome in a/j mice. J. Virol. **80:**10382–10394.
3. **Ding, Y., H. Wang, H. Shen, Z. Li, J. Geng, H. Han, J. Cai, X. Li, W. Kang, D. Weng, Y. Lu, D. Wu, L. He, and K. Yao.** 2003. The clinical pathology of severe acute respiratory syndrome (SARS): a report from China. J. Pathol. **200:**282–289.
4. **Duniho, S. M., J. Martin, J. S. Forster, M. B. Cascio, T. S. Moran, L. B. Carpin, and A. M. Sciuto.** 2002. Acute changes in lung histopathology and bronchoalveolar lavage parameters in mice exposed to the choking agent gas phosgene. Toxicol. Pathol. **30:**339–349.
5. **Ely, K. H., A. D. Roberts, J. E. Kohlmeier, M. A. Blackman, and D. L. Woodland.** 2007. Aging and $CD8^+$ T cell immunity to respiratory virus infections. Exp. Gerontol. **42:**427–431.
6. **Fleming, J. O., M. D. Trousdale, J. Bradbury, S. A. Stohlman, and L. P. Weiner.** 1987. Experimental demyelination induced by coronavirus JHM (MHV-4): molecular identification of a viral determinant of paralytic disease. Microb. Pathog. **3:**9–20.
7. **Fleming, J. O., M. D. Trousdale, F. A. el-Zaatari, S. A. Stohlman, and L. P. Weiner.** 1986. Pathogenicity of antigenic variants of murine coronavirus JHM selected with monoclonal antibodies. J. Virol. **58:**869–875.
8. **Fouchier, R. A., T. Kuiken, M. Schutten, G. van Amerongen, G. J. van Doornum, B. G. van den Hoogen, M. Peiris, W. Lim, K. Stohr, and A. D. Osterhaus.** 2003. Aetiology: Koch's postulates fulfilled for SARS virus. Nature **423:**240.
9. **Franks, T. J., P. Y. Chong, P. Chui, J. R. Galvin, R. M. Lourens, A. H. Reid, E. Selbs, C. P. McEvoy, C. D. Hayden, J. Fukuoka, J. K. Taubenberger, and W. D. Travis.** 2003. Lung pathology of severe acute respiratory syndrome (SARS): a study of 8 autopsy cases from Singapore. Hum. Pathol. **34:**743–748.
10. **Gallagher, T. M.** 1996. Murine coronavirus membrane fusion is blocked by modification of thiols buried within the spike protein. J. Virol. **70:**4683–4690.
11. **Glass, W. G., K. Subbarao, B. Murphy, and P. M. Murphy.** 2004. Mechanisms of host defense following severe acute respiratory syndrome-coronavirus (SARS-CoV) pulmonary infection of mice. J. Immunol. **173:**4030–4039.
12. **Gledhill, A. W., C. H. Andrewes, and G. W. Dick.** 1952. Production of hepatitis in mice by the combined action of two filterable agents. Lancet **ii:**509–511.
13. **Hamelmann, E., J. Schwarze, K. Takeda, A. Oshiba, G. L. Larsen, C. G. Irvin, and E. W. Gelfand.** 1997. Noninvasive measurement of airway responsiveness in allergic mice using barometric plethysmography. Am. J. Respir. Crit. Care Med. **156:**766–775.
14. **Harrod, K. S., R. J. Jaramillo, J. A. Berger, A. P. Gigliotti, S. K. Seilkop, and M. D. Reed.** 2005. Inhaled diesel engine emissions reduce bacterial clearance and exacerbate lung disease to *Pseudomonas aeruginosa* infection in vivo. Toxicol. Sci. **83:**155–165.
15. **Haynes, L., and S. L. Swain.** 2006. Why aging T cells fail: implications for vaccination. Immunity **24:**663–666.
16. **Hogan, R. J., G. Gao, T. Rowe, P. Bell, D. Flieder, J. Paragas, G. P. Kobinger, N. A. Wivel, R. G. Crystal, J. Boyer, H. Feldmann, T. G. Voss, and J. M. Wilson.** 2004. Resolution of primary severe acute respiratory syndrome-associated coronavirus infection requires Stat1. J. Virol. **78:**11416–11421.
17. **Holmes, K. V.** 2003. SARS-associated coronavirus. N. Engl. J. Med. **348:**1948–1951.
18. **Houtman, J. J., and J. O. Fleming.** 1996. Pathogenesis of mouse hepatitis virus-induced demyelination. J. Neurovirol. **2:**361–376.
19. **Hussell, T., A. Pennycook, and P. J. M. Openshaw.** 2001. Inhibition of tumor necrosis factor reduces the severity of virus-specific lung immunopathology. Eur. J. Immunol. **31:**2566–2573.
20. **Imai, Y., K. Kuba, G. G. Neely, R. Yaghubian-Malhami, T. Perkmann, G. van Loo, M. Ermolaeva, R. Veldhuizen, Y. H. Leung, H. Wang, H. Liu, Y. Sun, M. Pasparakis, M. Kopf, C. Mech, S. Bavari, J. S. Peiris, A. S. Slutsky, S. Akira, M. Hultqvist, R. Holmdahl, J. Nicholls, C. Jiang, C. J. Binder, and J. M. Penninger.** 2008. Identification of oxidative stress and Toll-like receptor 4 signaling as a key pathway of acute lung injury. Cell **133:**235–249.
21. **Knobler, R. L., P. W. Lampert, and M. B. Oldstone.** 1982. Virus persistence and recurring demyelination produced by a temperature-sensitive mutant of MHV-4. Nature **298:**279–280.
22. **Ksiazek, T. G., D. Erdman, C. S. Goldsmith, S. R. Zaki, T. Peret, S. Emery, S. Tong, C. Urbani, J. A. Comer, W. Lim, P. E. Rollin, S. F. Dowell, A. E. Ling, C. D. Humphrey, W. J. Shieh, J. Guarner, C. D. Paddock, P. Rota, B. Fields, J. DeRisi, J. Y. Yang, N. Cox, J. M. Hughes, J. W. LeDuc, W. J. Bellini, and L. J. Anderson.** 2003. A novel coronavirus associated with severe acute respiratory syndrome. N. Engl. J. Med. **348:**1953–1966.
23. **Lavi, E., D. H. Gilden, Z. Wroblewska, L. B. Rorke, and S. R. Weiss.** 1984. Experimental demyelination produced by the A59 strain of mouse hepatitis virus. Neurology **34:**597–603.
24. **Lee, N., D. Hui, A. Wu, P. Chan, P. Cameron, G. M. Joynt, A. Ahuja, M. Y. Yung, C. B. Leung, K. F. To, S. F. Lui, C. C. Szeto, S. Chung, and J. J. Sung.** 2003. A major outbreak of severe acute respiratory syndrome in Hong Kong. N. Engl. J. Med. **348:**1986–1994.
25. **Li, W., Z. Shi, M. Yu, W. Ren, C. Smith, J. H. Epstein, H. Wang, G. Crameri, Z. Hu, H. Zhang, J. Zhang, J. McEachern, H. Field, P. Daszak, B. T. Eaton,**

S. Zhang, and L. F. Wang. 2005. Bats are natural reservoirs of SARS-like coronaviruses. Science **310:**676–679.

26. **Mandelberg, A., G. Tal, L. Naugolny, K. Cesar, A. Oron, S. Houri, E. Gilad, and E. Somekh.** 2006. Lipopolysaccharide hyporesponsiveness as a risk factor for intensive care unit hospitalization in infants with respiratory syncytial virus bronchiolitis. Clin. Exp. Immunol. **144:**48–52.
27. **Marra, M. A., S. J. Jones, C. R. Astell, R. A. Holt, A. Brooks-Wilson, Y. S. Butterfield, J. Khattra, J. K. Asano, S. A. Barber, S. Y. Chan, A. Cloutier, S. M. Coughlin, D. Freeman, N. Girn, O. L. Griffith, S. R. Leach, M. Mayo, H. McDonald, S. B. Montgomery, P. K. Pandoh, A. S. Petrescu, A. G. Robertson, J. E. Schein, A. Siddiqui, D. E. Smailus, J. M. Stott, G. S. Yang, F. Plummer, A. Andonov, H. Artsob, N. Bastien, K. Bernard, T. F. Booth, D. Bowness, M. Czub, M. Drebot, L. Fernando, R. Flick, M. Garbutt, M. Gray, A. Grolla, S. Jones, H. Feldmann, A. Meyers, A. Kabani, Y. Li, S. Normand, U. Stroher, G. A. Tipples, S. Tyler, R. Vogrig, D. Ward, B. Watson, R. C. Brunham, M. Krajden, M. Petric, D. M. Skowronski, C. Upton, and R. L. Roper.** 2003. The Genome sequence of the SARS-associated coronavirus. Science **300:**1399–1404.
28. **Nagata, N., N. Iwata, H. Hasegawa, S. Fukushi, A. Harashima, Y. Sato, M. Saijo, F. Taguchi, S. Morikawa, and T. Sata.** 2008. Mouse-passaged severe acute respiratory syndrome-associated coronavirus leads to lethal pulmonary edema and diffuse alveolar damage in adult but not young mice. Am. J. Pathol. **172:**1625–1637.
29. **Nicholls, J. M., L. L. Poon, K. C. Lee, W. F. Ng, S. T. Lai, C. Y. Leung, C. M. Chu, P. K. Hui, K. L. Mak, W. Lim, K. W. Yan, K. H. Chan, N. C. Tsang, Y. Guan, K. Y. Yuen, and J. S. Peiris.** 2003. Lung pathology of fatal severe acute respiratory syndrome. Lancet **361:**1773–1778.
30. **Olson, M. R., and S. M. Varga.** 2007. CD8 T cells inhibit respiratory syncytial virus (RSV) vaccine-enhanced disease. J. Immunol. **179:**5415–5424.
31. **Poltorak, A., X. He, I. Smirnova, M. Y. Liu, C. Van Huffel, X. Du, D. Birdwell, E. Alejos, M. Silva, C. Galanos, M. Freudenberg, P. Ricciardi-Castagnoli, B. Layton, and B. Beutler.** 1998. Defective LPS signaling in C3H/HeJ and C57BL/10ScCr mice: mutations in Tlr4 gene. Science **282:** 2085–2088.
32. **Poutanen, S. M., D. E. Low, B. Henry, S. Finkelstein, D. Rose, K. Green, R. Tellier, R. Draker, D. Adachi, M. Ayers, A. K. Chan, D. M. Skowronski, I. Salit, A. E. Simor, A. S. Slutsky, P. W. Doyle, M. Krajden, M. Petric, R. C. Brunham, and A. J. McGeer.** 2003. Identification of severe acute respiratory syndrome in Canada. N. Engl. J. Med. **348:**1995–2005.
33. **Puthothu, B., J. Forster, A. Heinzmann, and M. Krueger.** 2006. TLR-4 and CD14 polymorphisms in respiratory syncytial virus associated disease. Dis. Markers **22:**303–308.
34. **Roberts, A., D. Deming, C. D. Paddock, A. Cheng, B. Yount, L. Vogel, B. D. Herman, T. Sheahan, M. Heise, G. L. Genrich, S. R. Zaki, R. Baric, and K. Subbarao.** 2007. A mouse-adapted SARS-coronavirus causes disease and mortality in BALB/c mice. PLoS Pathog. **3:**e5.
35. **Roberts, A., E. W. Lamirande, L. Vogel, J. P. Jackson, C. D. Paddock, J. Guarner, S. R. Zaki, T. Sheahan, R. Baric, and K. Subbarao.** 2008. Animal models and vaccines for SARS-CoV infection. Virus Res. **133:**20–32.
36. **Roberts, A., C. Paddock, L. Vogel, E. Butler, S. Zaki, and K. Subbarao.** 2005. Aged BALB/c mice as a model for increased severity of severe acute respiratory syndrome in elderly humans. J. Virol. **79:**5833–5838.
37. **Rota, P. A., M. S. Oberste, S. S. Monroe, W. A. Nix, R. Campagnoli, J. P. Icenogle, S. Penaranda, B. Bankamp, K. Maher, M. H. Chen, S. Tong, A. Tamin, L. Lowe, M. Frace, J. L. DeRisi, Q. Chen, D. Wang, D. D. Erdman, T. C. Peret, C. Burns, T. G. Ksiazek, P. E. Rollin, A. Sanchez, S. Liffick, B. Holloway, J. Limor, K. McCaustland, M. Olsen-Rasmussen, R. Fouchier, S. Gunther, A. D. Osterhaus, C. Drosten, M. A. Pallansch, L. J. Anderson, and W. J. Bellini.** 2003. Characterization of a novel coronavirus associated with severe acute respiratory syndrome. Science **300:**1394–1399.
38. **Singh, B., K. Shinagawa, C. Taube, E. W. Gelfand, and R. Pabst.** 2005. Strain-specific differences in perivascular inflammation in lungs in two murine models of allergic airway inflammation. Clin. Exp. Immunol. **141:**223–229.
39. **Snijder, E. J., P. J. Bredenbeek, J. C. Dobbe, V. Thiel, J. Ziebuhr, L. L. Poon, Y. Guan, M. Rozanov, W. J. Spaan, and A. E. Gorbalenya.** 2003. Unique and conserved features of genome and proteome of SARS-coronavirus, an early split-off from the coronavirus group 2 lineage. J. Mol. Biol. **331:**991–1004.
40. **Stohlman, S. A., P. R. Brayton, J. O. Fleming, L. P. Weiner, and M. M. Lai.** 1982. Murine coronaviruses: isolation and characterization of two plaque morphology variants of the JHM neurotropic strain. J. Gen. Virol. **63:**265–275.
41. **Subbarao, K., J. McAuliffe, L. Vogel, G. Fahle, S. Fischer, K. Tatti, M. Packard, W. J. Shieh, S. Zaki, and B. Murphy.** 2004. Prior infection and passive transfer of neutralizing antibody prevent replication of severe acute respiratory syndrome coronavirus in the respiratory tract of mice. J. Virol. **78:**3572–3577.
42. **Tal, G., A. Mandelberg, I. Dalal, K. Cesar, E. Somekh, A. Tal, A. Oron, S. Itskovich, A. Ballin, S. Houri, A. Beigelman, O. Lider, G. Rechavi, and N. Amariglio.** 2004. Association between common Toll-like receptor 4 mutations and severe respiratory syncytial virus disease. J. Infect. Dis. **189:**2057–2063.
43. **Tse, G. M., K. F. To, P. K. Chan, A. W. Lo, K. C. Ng, A. Wu, N. Lee, H. C. Wong, S. M. Mak, K. F. Chan, D. S. Hui, J. J. Sung, and H. K. Ng.** 2004. Pulmonary pathological features in coronavirus associated severe acute respiratory syndrome (SARS). J. Clin. Pathol. **57:**260–265.
44. **Van Der Hoek, L., K. Pyrc, M. F. Jebbink, W. Vermeulen-Oost, R. J. Berkhout, K. C. Wolthers, P. M. Wertheim-Van Dillen, J. Kaandorp, J. Spaargaren, and B. Berkhout.** 2004. Identification of a new human coronavirus. Nat. Med. **10:**368–373.
45. **Vogel, S. N., C. T. Hansen, and D. L. Rosenstreich.** 1979. Characterization of a congenitally LPS-resistant, athymic mouse strain. J. Immunol. **122:**619–622.
46. **Woo, P. C., S. K. Lau, C. M. Chu, K. H. Chan, H. W. Tsoi, Y. Huang, B. H. Wong, R. W. Poon, J. J. Cai, W. K. Luk, L. L. Poon, S. S. Wong, Y. Guan, J. S. Peiris, and K. Y. Yuen.** 2005. Characterization and complete genome sequence of a novel coronavirus, coronavirus HKU1, from patients with pneumonia. J. Virol. **79:**884–895.
47. **Zhao, Z., F. Zhang, M. Xu, K. Huang, W. Zhong, W. Cai, Z. Yin, S. Huang, Z. Deng, M. Wei, J. Xiong, and P. M. Hawkey.** 2003. Description and clinical treatment of an early outbreak of severe acute respiratory syndrome (SARS) in Guangzhou, PR China. J. Med. Microbiol. **52:**715–720.
48. **Zhong, N. S., B. J. Zheng, Y. M. Li, L. L. M. Poon, Z. H. Xie, K. H. Chan, P. H. Li, S. Y. Tan, Q. Chang, J. P. Xie, X. Q. Liu, J. Xu, D. X. Li, K. Y. Yuen, J. S. M. Peiris, and Y. Guan.** 2003. Epidemiology and cause of severe acute respiratory syndrome (SARS) in Guangdong, People's Republic of China, in February, 2003. Lancet **362:**1353–1358.